<b>Regional-scale jet waviness modulates the occurrence</b>	e of
mid-latitude weather extremes	

### Matthias Röthlisberger<sup>1</sup>, Stephan Pfahl<sup>2</sup>and Olivia Martius<sup>1,3</sup>

4	<sup>1</sup> Oeschger Centre for Climate Change Research and Institute of Geography, University of Bern, Bern, Switzerland
5	<sup>2</sup> Institute for Atmospheric and Climate Science, ETH Zürich, Zürich, Switzerland
6	<sup>3</sup> Mobiliar Lab for Natural Risks, University of Bern, Bern, Switzerland

#### Key Points:

1

3

7

12

# Regional-scale jet waviness significantly modulates the number and location of weather extremes Weather extremes are primarily affected by regional-scale rather than hemispheric jet waviness

• The strength and sign of the waviness-extremes link differs between regions

Corresponding author: Matthias Röthlisberger, matthias.roethlisberger@giub.unibe.ch

#### 13 Abstract

Several studies have attributed the occurrence of recent weather extremes to an amplified wavi-14 ness of the upper-tropospheric jet stream. Although trends in jet waviness are still under dis-15 cussion, it is crucial to better understand the mechanisms through which jet waviness affects 16 weather extremes. Here we show that variations in jet waviness on regional scales effectively 17 modulate the occurrence of daily weather extremes, however, in regionally different ways. The 18 jet waviness over the North Atlantic and the North Pacific mainly affects where wind, precip-19 itation and cold extremes occur, while a wavy jet over Eurasia strongly favors the occurrence 20 of hot extremes in summer. This is because regional variations of jet waviness are intrinsically 21 linked to the occurrence and tracks of synoptic-scale weather systems, which can trigger the 22 extremes. We conclude that potential jet waviness changes would affect the occurrence of weather 23 extremes differently depending on where these changes occur. 24

#### **1 Introduction**

In recent years the Northern Hemisphere mid-latitudes have been hit by a remarkable 26 series of high-impact weather extremes including the record breaking heat waves in Europe 27 in 2003 [Black et al., 2004] and in Russia in 2010 [Barriopedro et al., 2011], severe floods in 28 the United Kingdom in 2013/2014 [Herring et al., 2014] and unusually cold winters with dev-29 astating winter storms in the eastern United States [Palmer, 2014; Vose et al., 2014]. The num-30 ber, diversity and severity of these weather extremes has triggered an engaged debate on the 31 causes of their temporally clustered occurrence. While a change in the frequency of some ex-32 tremes is expected with global warming [IPCC, 2012; Coumou and Rahmstorf, 2012; Schnei-33 der et al., 2015; Hoskins and Woollings, 2015], most studies agree that the recent series of mid-34 latitude weather extremes cannot be explained by the observed shift in the mean temperature 35 and thermodynamic arguments alone [Horton et al., 2015]. Hence, these weather extremes must 36 at least partly be related to anomalous atmospheric circulation patterns [Horton et al., 2015; 37 Hoskins and Woollings, 2015]. 38

Several studies have proposed that increased waviness of the polar jet has favored the occurrence of particular weather extremes [*Francis and Vavrus*, 2012; *Petoukhov et al.*, 2013; *Screen and Simmonds*, 2014; *Francis and Vavrus*, 2015; *Francis and Skific*, 2015]. Previous studies investigating this "waviness-extremes" link have mainly focused on long-lasting extremes on continental to hemispheric scales [*Liu et al.*, 2012; *Petoukhov et al.*, 2013; *Coumou et al.*, 2014; *Screen and Simmonds*, 2014]. Statistically significant links between jet waviness on a

-2-

hemispheric scale and monthly temperature and precipitation extremes could be established
 for several mid-latitude regions [*Screen and Simmonds*, 2014]. On synoptic (multi-day) time scales, periods of frequently occurring temperature and precipitation extremes have recently
 been linked to low- and high storm track activity, respectively [*Lehmann and Coumou*, 2015;
 *Coumou et al.*, 2015]. However, one particularly important aspect of this topic has not been
 investigate so far, namely regional variations in the strength and sign of this link.

A variety of jet waviness measures have been proposed in recent studies. Some of them 51 conceptualize jet waviness as the amplitudes of the excursions of geopotential height isopleths 52 or isentropic PV contours from a zonal background state [Francis and Vavrus, 2012, 2015; Screen 53 and Simmonds, 2013a; Röthlisberger et al., 2016]. Others rely on Fourier analysis of the merid-54 ional wind or the geopotential height in particular latitude bands [Petoukhov et al., 2013; Coumou 55 et al., 2014; Screen and Simmonds, 2013a, 2014] as an indication for wave amplitudes. The 56 use of these conceptually different types of waviness measures may lead to contradicting re-57 sults, as a number of studies has shown that trends in jet waviness as inferred from these dif-58 ferent measures do not generally agree [Barnes, 2013; Barnes and Screen, 2015; Screen and 59 Simmonds, 2013b]. 60

Here, we use the regional-scale jet waviness measure introduced by *Röthlisberger et al.* [2016] only to discriminate between regionally wavy and zonal upper-level flow configurations and investigate, where and how a regionally wavy (or zonal) jet favors or hampers the occurrence of daily weather extremes.

It is well established that mid-latitude weather extremes often occur in association with 65 synoptic-scale weather systems such as cyclones and blocking anticyclones and that these weather 66 systems are steered by the upper-level flow [e.g., Dickson and Namias, 1976; Davies, 2015]. 67 For example precipitation and wind extremes in winter occur preferentially in or near extra-68 tropical cyclones [Donat et al., 2010; Pfahl and Wernli, 2012a; Vose et al., 2014]. Winter cold 69 extremes in western Europe and the Mediterranean often occur during cold air outbreaks down-70 stream of North Atlantic blocking [Sillmann et al., 2011; Buehler et al., 2011] and in the same 71 way blocking over the North Pacific favors cold extremes in western North America [Whan 72 et al., 2016]. Summer heat extremes, in contrast, tend to occur near the center of blocking an-73 ticyclones [Pfahl and Wernli, 2012b], mainly for two reasons: Firstly, subsiding air within the 74 blocks and the resulting clear sky conditions lead to increased solar irradiation reaching the 75 Earth's surface [Black et al., 2004; Barriopedro et al., 2011; Pfahl and Wernli, 2012b]. Sec-76

-3-

ondly, the adiabatic warming of the subsiding air leads to reduced relative humidity and prevents precipitation. The lack of precipitation as well as the increased solar irradiation both contribute to soil moisture depletion which in turn increases the surface sensible heat flux [e.g., *Namias*, 1960; *Fischer et al.*, 2007; *Seneviratne et al.*, 2010]. Over the oceans the influence of
blocking on extreme temperature is much reduced, on the one hand due to the larger heat capacity compared to the land surface (and hence less temperature variability on synoptic time
scales) but also due to the lack of the soil-moisture coupling [*Pfahl and Wernli*, 2012b].

From a meteorological point of view it is therefore clear that weather systems are cru-84 cial for understanding the waviness-extremes link. However, in the recent literature their piv-85 otal role in linking the upper-level flow to surface weather extremes has not been considered 86 sufficiently. In this study we thus aim to contribute to this current discussion in two ways: Firstly, 87 we analyze this waviness-extremes link regionally and show that the strength and sign of this 88 link varies between regions and types of extremes. Secondly, we use feature based climatolo-89 gies of extratropical cyclones and blocking anticyclones to illustrate the regionally varying role 90 of weather systems in linking jet waviness to the occurrence of surface weather extremes. 91

#### 92 **2** Data and Methods

93

#### 2.1 Extremes and Jet Waviness Data

The ERA-Interim re-analysis data set [Dee et al., 2011] (interpolated to 1°×1° hori-94 zontal resolution, covering the period of 1979-2012) is used to identify daily extremes of daily 95 maximum 10 m wind gusts (ERA-Interim variable "10 metre wind gust since previous post-96 processing"), daily maximum 2 m temperature, daily minimum 2 m temperature and daily ac-97 cumulated precipitation as the 5% most extreme values per season at every grid point. These 98 data stem from short term model predictions (with lead times between 6 and 18 h) of the Eu-99 ropean Centre for Medium-Range Weather Forecasts (ECMWF) Integrated Forecast System 100 (IFS) model which was used for producing the ERA-Interim data set. Note that the absolute 101 values of the extremes are largely irrelevant for our analysis. Rather it is the timing of the ex-102 treme events that matters for this analysis and previous studies have reported that in the ex-103 tratropics this timing is reasonably well represented in ERA-Interim [Pfahl and Wernli, 2012a]. 104

The waviness of the polar jet is measured separately in the Eurasian ( $0^{\circ}E-135^{\circ}E$ ), North Pacific ( $135^{\circ}E-120^{\circ}W$ ), North American ( $120^{\circ}W-60^{\circ}W$ ) and North Atlantic ( $60^{\circ}W-0^{\circ}E$ ) sectors using the jet waviness measure introduced by *Röthlisberger et al.* [2016]. This wavi-

-4-

ness measure is based on isentropic potential vorticity (PV) fields from ERA-Interim (on the 108 320 K isentrope in winter and on 335 K in summer), and uses the geometry of the 2 potential 109 vorticity unit (PVU) contours on these isentropes as an indicator for the waviness of the po-110 lar jet. The 2 PVU contour (i.e., the dynamical tropopause) on these isentropes is co-located 111 with the polar jet and hence the contour geometry is an excellent indicator for the waviness 112 of the polar jet. The jet waviness of a particular longitudinal sector is calculated by integrat-113 ing absolute values of latitude changes of the 2 PVU contour along this contour over the length 114 of the sector. High waviness results from large-amplitude meridional meanders of the polar 115 jet, while low waviness is obtained for zonally orientated jet segments. The waviness values 116 are calculated from 6-hourly PV fields and then averaged to obtain daily waviness time se-117 ries covering the period 1979-2012 for all sectors. High (low) waviness days for a particular 118 sector are defined as days on which the respective waviness value falls into the highest (low-119 est) quartile of the waviness distribution of the respective season and sector. The technical de-120 tails of the waviness measure are described in Supporting Text S1 [Martius et al., 2010]. 121

122

#### 2.2 Odds Ratios

Using these extremes and jet waviness data, the odds ratio (OR) of the occurrence of 123 an extreme during high (low) waviness in a particular sector is calculated at each grid point 124 125 as

$$OR = \frac{P(Ext|Wave)(1 - P(Ext))}{P(Ext)(1 - P(Ext|Wave))}$$
(1)

where P(Ext|Wave) is the probability of observing an extreme at the respective grid 126 point during a day with high (low) waviness, estimated as the number of high (low) waviness 127 days with a co-occurring extreme divided by the total number of high (low) waviness days. 128 P(Ext) is the probability of observing an extreme at any day, i.e., 0.05. With this approach 129 we thus assess, how frequently weather extremes co-occur with a regionally wavy (or zonal) 130 jet compared to their climatological frequency (see Stephenson [2000] and Chapter 8.2.2 in 131 Wilks [2011] for a discussion of the use of odds ratios in atmospheric sciences). 132

The significance of the ORs is assessed in a two step approach. First, a Monte-Carlo method 133 is applied to estimate *p*-values of the ORs at each grid point. Random waviness time series 134 are constructed for each region and season by shuffling the 34 seasons of the original time se-135 ries and connecting these shuffled seasons to a random 34-season waviness time series. This 136

shuffling of entire seasons is necessary, as for some sectors, the original waviness time series 137 exhibit substantial sub-seasonal variability, which, if not taken into account, strongly affects 138 the resulting *p*-values. By shuffling entire seasons, however, we ensure that the random time 139 series retain the autocorrelation and sub-seasonal variability of the original waviness data. This 140 procedure is repeated 1000 times, and p-values at each grid point are estimated through com-141 parison with the distribution of ORs from these samples. In a second step, the False Discov-142 ery Rate (FDR) test by *Benjamini and Hochberg* [1995] is applied to the entire set of *p*-values 143 from a given OR field. This test controls the number of falsely rejected null hypotheses in mul-144 tiple statistical testing. A maximum false discovery rate of 5% is chosen here. Note that, while 145 this test was originally developed for independent data, Ventura et al. [2004] have shown that 146 it also correctly controls the number of falsely rejected hypotheses in applications with spa-147 tially correlated climatological data. 148

149

#### 2.3 Blocking and Extratropical Cyclone Climatologies

To interpret the OR fields we incorporate objective climatologies of atmospheric blocking and extratropical cyclones into our analysis. We use the algorithm developed by *Schwierz et al.* [2004] to compile a climatology of atmospheric blocking and an updated version of the cyclone climatology of *Wernli and Schwierz* [2006] (see Supporting Texts S2 and S3 for descriptions of the identification algorithms). The seasonal climatologies of atmospheric blocking and extratropical cyclones are shown in Supporting Figure 1.

#### **3 Results and Discussion**

# 157

## 3.1 Spatially Aggregated Effect of Regional-Scale and Hemispheric Jet Waviness on Weather Extremes

We first discuss the effect of linking regional-scale rather than hemispheric jet waviness 159 with the extremes. Previous studies found that prolonged weather extremes, especially over 160 land areas, occur more frequently during periods with high jet waviness on a hemispheric scale 161 [Liu et al., 2012; Petoukhov et al., 2013; Coumou et al., 2014; Screen and Simmonds, 2014]. 162 Here we investigate, whether high regional-scale jet waviness is also consistently linked to more 163 extremes. Figure 1 depicts the size of the northern hemisphere land area with significant ORs 164 for high waviness and all four types of extremes. For high waviness, the majority of the sig-165 nificant ORs is larger than one, while the opposite is true for low jet waviness (Supporting Fig-166

-6-

<sup>167</sup> ure 2). Thus, there is a general tendency for more daily wind, precipitation, cold and hot ex-<sup>168</sup> tremes when the jet is regionally wavy. Locally, though, the opposite may be the case; for ex-<sup>169</sup> ample the odds of winter cold extremes over western Canada and Alaska are decreased when <sup>170</sup> the jet is wavy in the North American sector (see Figures 1 and 3, Supporting Figure 3 and <sup>171</sup> discussion in Section 3.3).

Carrying out the same analysis for hemispheric jet waviness shows that for both high and low waviness, the land area of significant ORs is smaller for hemispheric than regionalscale jet waviness (Figure 1, Supporting Figure 2). Hence, daily weather extremes are affected primarily by regional-scale rather than hemispheric jet waviness. We next study the link between regional-scale jet waviness and extremes in more detail to show why the link is stronger on regional scales and which flow configurations and synoptic weather patterns contribute to the extremes.

179

#### 3.2 Precipitation and Wind Extremes

We start with the ORs of winter (December-February, DJF) precipitation and wind ex-180 tremes for high waviness in the North Atlantic sector (Figure 2(a,b)). A wavy North Atlantic 181 jet is associated with more frequent precipitation and wind extremes over northeastern Canada, 182 Greenland and off the coast of Morocco (odds increased by 50-150%), while over the British 183 Isles and parts of western Europe precipitation and wind extremes are less frequent (odds re-184 duced by up to 75%). Moreover, a wavy North Atlantic jet is associated with more cyclones 185 between Newfoundland and Greenland and off the coast of Morocco, as well as a reduced cy-186 clone frequency in the northeastern North Atlantic (Figure 2(a,b)). 187

The modulation of the cyclone frequencies explains the spatial patterns of the wind and 188 precipitation extreme ORs: as expected from prior knowledge, wind and precipitation extremes 189 are more frequent in areas with more cyclones. This is further illustrated for two grid points 190 located in the areas of high OR over the Davis Strait at 57 °W/62 °N and over the eastern sub-191 tropical Atlantic at 15 °W/32 °N (Figure 2(c,d)). Precipitation extremes over the Davis Strait 192 during winter are associated with a cyclonically overturning dynamical tropopause, i.e. cyclonic 193 Rossby wave breaking, over the western North Atlantic, which produces the high waviness sig-194 nal (Figure 2(c)). More frequent extratropical cyclones over Baffin Island and very high amounts 195 of moisture favor the occurrence of precipitation extremes (Figure 2(c)). The synoptic situ-196 ation for wind extremes over the Davis Strait is similar (Supporting Figure S4). Precipitation 197

-7-

extremes over the subtropical eastern Atlantic occur during anticyclonic Rossby wave break-198 ing events over the subtropical Atlantic (Figure 2(d)) and are associated with an enhanced cy-199 clone frequency as well as increased atmospheric moisture content in the area of the precip-200 itation extremes. These two composites illustrate a pivotal difficulty that arises when study-201 ing the link between jet waviness and weather extremes: The high waviness days contain sev-202 eral distinct synoptic flow configurations, even for relatively small longitudinal sectors, and 203 extremes in different areas of significant ORs do not necessarily occur on the same day. The 204 statistical analyses only pick up the most dominant of these flow configurations. Considering 205 hemispheric waviness thus leads to a strong "smoothing" of the synoptic link to the extremes 206 and hence less statistically significant ORs. 207

Results for other sectors and seasons further emphasize the key role of weather systems 208 in linking jet waviness to precipitation and wind extremes. For North Pacific jet waviness, OR 209 patterns are qualitatively similar to those for the North Atlantic (Supporting Figure 5). For high 210 Eurasian jet waviness significant ORs of wind and precipitation extremes are confined to the 211 Asian high Arctic (Supporting Figure 6), where these extremes are favored by high jet wavi-212 ness. In regions where extratropical cyclones occur less frequently (Supporting Figure 1) ORs 213 of wind and precipitation extremes for high Eurasian jet waviness are similar to climatology 214 (Supporting Figure 6). During the summer months (July-August, JJA) OR patterns for wind 215 and precipitation extremes are qualitatively similar to winter (Supporting Figure 7), however, 216 the signals are weaker, conceivably due to the reduced number and intensity of extratropical 217 cyclones [Wernli and Schwierz, 2006] and more extremes occurring in association with smaller 218 scale processes such as convection. 219

220

#### 3.3 Cold Extremes

We next look at cold extremes during DJF in the Atlantic sector (Figure 3(a)). A wavy 221 North Atlantic jet is associated with more frequent blocking situations over the central North 222 Atlantic and an increased number of cold extremes downstream in western Europe and parts 223 of the Mediterranean (Figure 3(a)). During days when cold extremes in western France at 4°W/48°N 224 co-occur with high North Atlantic waviness, the blocking frequency is increased over the North 225 Atlantic and easterly and northeasterly winds advect cold air to western Europe (i.e., to the 226 south and downstream of the blocks, Figure 3(d)). This is in good agreement with previous 227 results of Sillmann et al. [2011] and Buehler et al. [2011]. There is also an area of significant 228 ORs in the subtropical Atlantic. Cold extremes in this region are related to an anticyclonic over-229

-8-

turning of the tropopause over the subtropical Atlantic with a trough reaching far southward
bringing the cold air into the subtropics (Figure 3(c)). This flow configuration is accompanied
by an anomalously high blocking frequency upstream and to the north, over the western Atlantic. Again cold extremes over the subtropical Atlantic and western Europe are linked to distinctly different, but all high waviness, upper-level flow configurations over the Atlantic.

Furthermore, a wavy jet over North America is associated with less frequent cold extremes over vast areas of western Canada and Alaska, as well as more frequent blocking over central Canada (Figure 3(b)). Hence, these reduced odds conceivably result from more frequent warm air advection and suppressed cold air advection in the western part of the blocks (see also Supporting Figure 3).

#### 240 **3.4 Hot Extremes**

Recent studies have suggested that changes in summer circulation might contribute significantly to a further increase in the number of hot extremes [*Francis and Vavrus*, 2012, 2015; *Horton et al.*, 2015; *Coumou et al.*, 2015], the hypothesis being that a more wavy jet stream is associated with more frequent atmospheric blocks [*Francis and Vavrus*, 2012; *Liu et al.*, 2012; *Francis and Vavrus*, 2015], which are conducive to summer hot extremes [*Black et al.*, 2004; *Barriopedro et al.*, 2011; *Pfahl and Wernli*, 2012b; *Horton et al.*, 2015].

Indeed, a regionally wavy jet over the Northern Hemisphere land masses favors the oc-247 currence of hot extremes (Figure 4). Over western Russia, for example, in the region where 248 the Russian heat wave in 2010 was most pronounced [Barriopedro et al., 2011], the odds of 249 summer hot extremes are increased by up to 150% during days with a wavy Eurasian jet (Fig-250 ure 4(a)). In the same area, the frequency of atmospheric blocking is increased by roughly 50% 251 compared to climatology (Figure 4(a) and Supporting Figure 1). A similar link is evident over 252 eastern Siberia and over North America, (Figure 4(a) and (b)), where a wavy jet in summer 253 favors more atmospheric blocking over Canada and is associated with more frequent hot ex-254 tremes south of the Baffin Bay. Over the oceans, however, the ORs of summer hot extremes 255 do not differ significantly from climatology during days with high regional-scale jet waviness 256 (Supporting Figure 8), which is consistent with the findings of *Pfahl and Wernli* [2012b], as 257 discussed in Section 1. 258

-9-

#### **4 Summary and Conclusions**

This study reveals a statistically highly significant and meteorologically explicable link 260 between regional-scale jet waviness and the occurrence of different types of daily mid-latitude 261 weather extremes. Regional-scale jet waviness affects daily weather extremes through its link-262 age to synoptic-scale weather systems (cyclones and blocking) that trigger the extremes. In 263 winter, the link between jet waviness and the occurrence of daily wind, precipitation and cold 264 extremes is strongest in and around the Northern Hemisphere storm tracks, where these ex-265 tremes occur mostly in association with synoptic-scale weather systems. Further away from 266 the storm tracks, the odds of daily wind, precipitation and cold extremes are not significantly 267 affected by regional-scale jet waviness. In summer, the waviness-extremes linkage weakens 268 for wind and precipitation extremes, however, high jet waviness over the continents strongly 269 enhances the number of hot extremes by favoring the occurrence of atmospheric blocking. 270

While the presented results are consistent with previous findings on the role of weather systems in triggering extremes, they also clearly show that the strength and sign of the wavinessextremes link varies depending on sector, season and type of extreme. This implies that if jet waviness is to change in regionally differing ways [*Francis and Vavrus*, 2012; *Screen and Simmonds*, 2013a; *Francis and Vavrus*, 2015; *Francis and Skific*, 2015], the implications for the occurrence of extremes will fundamentally depend on where jet waviness changes occur.

Compared to previous studies that investigated the linkage of weather extremes to hemispheric jet waviness [*Liu et al.*, 2012; *Petoukhov et al.*, 2013; *Coumou et al.*, 2014; *Screen and Simmonds*, 2014], the regional-scale waviness measure used here, enables clearer and more significant associations with weather extremes. In addition, the meteorological mechanisms responsible for this linkage are shown by incorporating changes in the frequency of synopticscale weather systems. Our findings have the following important implications for the discussion of altered weather extremes due to changes in jet waviness.

- The link between jet waviness and the occurrence of weather extremes is stronger for
   regional-scale than hemispheric jet waviness and also varies between regions. Hence,
   waviness changes on regional scales are more relevant for changes in the frequency of
   weather extremes than changes in hemispheric jet waviness. Therefore, potential changes
   in jet waviness need to be identified regionally.
- 289
   2. Jet waviness is linked to the occurrence of daily weather extremes via synoptic-scale
   290 weather systems. To understand future changes in the occurrence of daily weather ex-

-10-

tremes in the mid-latitudes, future research needs to assess how climate change affects the number, intensity and pathway of synoptic-scale weather systems as well as their ability to trigger extremes.

#### 294 Acknowledgments

- <sup>295</sup> The authors thank the ECMWF for providing access to the ERA-Interim data, R. Beerli (ETH
- Zürich) for helpful discussions about hypothesis testing and two reviewers which helped greatly
- to improve the clarity of this manuscript. M.R. wishes to acknowledge the Swiss National Sci-
- ence foundation for its financial support (Grant number 200021\_159905/1). ERA-Interim data
- can be accessed under http://apps.ecmwf.int/datasets/data/interim-full-daily.

#### 300 References

- Barnes, E. A. (2013), Revisiting the evidence linking Arctic amplification to extreme
- weather in midlatitudes, *Geophys. Res. Lett.*, 40, 4734–4739, doi:10.1002/grl.50880.
- Barnes, E. A., and J. A. Screen (2015), The impact of Arctic warming on the midlatitude
- jet-stream: Can it? Has it? Will it?, *Wiley Interdiscip. Rev. Clim. Chang.*, *6*, 277–286,
   doi:10.1002/wcc.337.
- Barriopedro, D., E. M. Fischer, J. Luterbacher, R. M. Trigo, and R. García-Herrera (2011),
   The hot summer of 2010: redrawing the temperature record map of Europe, *Science*,
   *332*, 220–224, doi:10.1126/science.1201224.
- Benjamini, Y., and Y. Hochberg (1995), Controlling the false discovery rate: a practical
- and powerful approach to multiple testing, J. Roy. Stat. Soc. B Met., 57, 289–300.
- Black, E., M. Blackburn, G. Harrison, B. Hoskins, and J. Methven (2004), Factors

contributing to the summer 2003 European heatwave, *Weather*, 59, 217–223, doi:
10.1256/wea.74.04.

- Buehler, T., C. C. Raible, and T. F. Stocker (2011), The relationship of winter season North Atlantic blocking frequencies to extreme cold or dry spells in the ERA-40, *Tellus*
- <sup>316</sup> A, 63, 212–222, doi:10.1111/j.1600-0870.2010.00492.x.
- Coumou, D., and S. Rahmstorf (2012), A decade of weather extremes, *Nat. Clim. Change*, 2, 491–496, doi:10.1038/nclimate1452.
- Coumou, D., V. Petoukhov, S. Rahmstorf, S. Petri, and H. J. Schellnhuber (2014),
- 320 Quasi-resonant circulation regimes and hemispheric synchronization of extreme
- weather in boreal summer, *P. Natl. Acad. Sci. USA*, 111, 12,331–12,336, doi:

322	10.1073/pnas.1412797111.

327

- Coumou, D., J. Lehmann, and J. Beckmann (2015), The weakening summer cir-323 culation in the Northern Hemisphere mid-latitudes, Science, 348, 324-327, doi: 324 10.1126/science.1261768. 325
- Davies, H. C. (2015), Weather chains during the 2013/2014 winter and their significance 326 for seasonal prediction, Nat. Geosci., 8, 833837, doi:10.1038/ngeo2561.
- Dee, D. P., S. M. Uppala, A. J. Simmons, P. Berrisford, P. Poli, S. Kobayashi, U. Andrae, 328
- M. A. Balmaseda, G. Balsamo, P. Bauer, P. Bechtold, A. C. M. Beljaars, L. van de 329
- Berg, J. Bidlot, N. Bormann, C. Delsol, R. Dragani, M. Fuentes, A. J. Geer, L. Haim-330
- berger, S. B. Healy, H. Hersbach, E. V. Hólm, L. Isaksen, P. Kallberg, M. Köhler, 331
- M. Matricardi, A. P. McNally, B. M. Monge-Sanz, J. J. Morcrette, B. K. Park, 332
- C. Peubey, P. de Rosnay, C. Tavolato, J. N. Thépaut, and F. Vitart (2011), The ERA-333
- Interim reanalysis: Configuration and performance of the data assimilation system, Q. J. 334
- Roy. Meteor. Soc., 137, 553-597, doi:10.1002/qj.828. 335
- Dickson, R. R., and J. Namias (1976), North American influences on the circulation and 336 climate of the North Atlantic sector, Mon. Weather Rev., 104(10), 1255-1265, doi: 337
- 10.1175/1520-0493(1976)104;1255:NAIOTC; 2.0.CO; 2. 338
- Donat, M. G., G. C. Leckebusch, J. G. Pinto, and U. Ulbrich (2010), Examination of wind 339 storms over Central Europe with respect to circulation weather types and NAO phases, 340 Int. J. Climatol., 30(9), 1289-1300, doi:10.1002/joc.1982. 341
- Fischer, E. M., S. Seneviratne, P. Vidale, D. Lüthi, and C. Schär (2007), Soil moisture-342
- atmosphere interactions during the 2003 European summer heat wave, J. Climate, 343
- 20(20), 5081-5099, doi:10.1175/JCLI4288.1. 344
- Francis, J., and N. Skific (2015), Evidence linking rapid Arctic warming to mid-latitude 345
- weather patterns, Phil. Trans. R. Soc. A, 373, 20140,170, doi:0.1098/rsta.2014.0170. 346
- Francis, J. A., and S. J. Vavrus (2012), Evidence linking Arctic amplification to extreme 347 weather in mid-latitudes, Geophys. Res. Lett., 39(6), doi:10.1029/2012GL051000. 348
- Francis, J. A., and S. J. Vavrus (2015), Evidence for a wavier jet stream in response to 349 rapid Arctic warming, Environ. Res. Lett., 10(1), doi:10.1088/1748-9326/10/1/014005. 350
- Herring, S. C., M. P. Hoerling, T. C. Peterson, and P. A. Stott (2014), Explaining extreme 351
- events of 2013 from a climate perspective, Bull. Amer. Meteorol. Soc., 95, S1-S104, 352
- doi:10.1175/1520-0477-95.9.S1.1. 353

354	Horton, D. E., N. C. Johnson, D. Singh, D. L. Swain, B. Rajaratnam, and N. S. Diffen-
355	baugh (2015), Contribution of changes in atmospheric circulation patterns to extreme
356	temperature trends, Nature, 522, 465-469, doi:10.1038/nature14550.
357	Hoskins, B. J., and T. Woollings (2015), Persistent extratropical regimes and climate ex-
358	tremes, Current Climate Change Reports, 1, 115-124, doi:10.1007/s40641-015-0020-8.
359	IPCC (2012), Managing the Risks of Extreme Events and Disasters to Advance Climate
360	Change Adaptation. A Special Report of Working Groups I and II of the Intergovernmental
361	Panel on Climate Change, 582 pp., Cambridge University Press.
362	Lehmann, J., and D. Coumou (2015), The influence of mid-latitude storm tracks on hot,
363	cold, dry and wet extremes, Sci. Rep., 5(17491), doi:10.1038/srep17491.
364	Liu, J., J. A. Curry, H. Wang, M. Song, and R. M. Horton (2012), Impact of declining
365	Arctic sea ice on winter snowfall, Proc. Natl. Acad. Sci. USA, 109, 4074-4079, doi:
366	10.1073/pnas.1114910109.
367	Martius, O., C. Schwierz, and H. C. Davies (2010), Tropopause-level waveguides, J.
368	Atmos. Sci., 67, 866-879, doi:10.1175/2009JAS2995.1.
369	Namias, J. (1960), Factors in the initiation, perpetuation and termination of drought, Inter-
370	national Association of Scientific Hydrology Commission on Surface Waters Publication,
371	51, 81–94.
372	Palmer, T. (2014), Record-breaking winters and global climate change, Science, 344,
373	803-804, doi:10.1126/science.1255147.
374	Petoukhov, V., S. Rahmstorf, S. Petri, and H. J. Schellnhuber (2013), Quasiresonant ampli-
375	fication of planetary waves and recent Northern Hemisphere weather extremes, P. Natl.
376	Acad. Sci. USA, 110, 5336–5341, doi:10.1073/pnas.1222000110.
377	Pfahl, S., and H. Wernli (2012a), Quantifying the relevance of cyclones for precipitation
378	extremes, J. Climate, 25, 6770-6780, doi:10.1175/JCLI-D-11-00705.1.
379	Pfahl, S., and H. Wernli (2012b), Quantifying the relevance of atmospheric blocking
380	for co-located temperature extremes in the Northern Hemisphere on (sub-) daily time
381	scales, Geophys. Res. Lett., 39(12), doi:10.1029/2012GL052261.
382	Röthlisberger, M., O. Martius, and H. Wernli (2016), An algorithm for identifying the
383	initiation of synoptic-scale Rossby waves on potential vorticity waveguides, Q. J. Roy.
384	Meteor. Soc., 142(695), 889–900, doi:10.1002/qj.2690.
385	Schneider, T., T. Bischoff, and H. Płotka (2015), Physics of changes in synoptic mid-
386	latitude temperature variability, J. Climate, 28, 2312-2331, doi:10.1175/JCLI-D-14-

387	00632.1.
388	Schwierz, C., M. Croci-Maspoli, and H. Davies (2004), Perspicacious indicators of atmo-
389	spheric blocking, Geophys. Res. Lett., 31(6), doi:10.1029/2003GL019341.
390	Screen, J. A., and I. Simmonds (2013a), Exploring links between Arctic amplification and
391	mid-latitude weather, Geophys. Res. Lett., 40, 959-964, doi:10.1002/grl.50174.
392	Screen, J. A., and I. Simmonds (2013b), Caution needed when linking weather extremes
393	to amplified planetary waves, Proceedings of the National Academy of Sciences, 110(26),
394	E2327-E2327, doi:10.1073/pnas.1304867110.
395	Screen, J. A., and I. Simmonds (2014), Amplified mid-latitude planetary waves
396	favour particular regional weather extremes, Nat. Clim. Change, 4, 704-709, doi:
397	10.1038/nclimate2271.
398	Seneviratne, S. I., T. Corti, E. L. Davin, M. Hirschi, E. B. Jaeger, I. Lehner, B. Or-
399	lowsky, and A. J. Teuling (2010), Investigating soil moisture-climate interactions
400	in a changing climate: A review, Earth-Science Reviews, 99(3), 125-161, doi:
401	10.1016/j.earscirev.2010.02.004.
402	Sillmann, J., M. Croci-Maspoli, M. Kallache, and R. W. Katz (2011), Extreme cold winter
403	temperatures in Europe under the influence of North Atlantic atmospheric blocking, J.
404	Climate, 24, 5899-5913, doi:10.1175/2011JCLI4075.1.
405	Stephenson, D. B. (2000), Use of the odds ratio for diagnosing forecast skill, Weather
406	Forecast., 15(2), 221–232, doi:10.1175/1520-0434(2000)015i0221:UOTORF¿2.0.CO;2.
407	Ventura, V., C. J. Paciorek, and J. S. Risbey (2004), Controlling the proportion of falsely
408	rejected hypotheses when conducting multiple tests with climatological data, J. Climate,
409	17, 4343–4356, doi:10.1175/3199.1.
410	Vose, R. S., S. Applequist, M. A. Bourassa, S. C. Pryor, R. J. Barthelmie, B. Blanton,
411	P. D. Bromirski, H. E. Brooks, A. T. DeGaetano, R. M. Dole, et al. (2014), Monitoring
412	and understanding changes in extremes: Extratropical storms, winds, and waves, Bull.
413	Amer. Meteorol. Soc., 95, 377-386, doi:10.1175/BAMS-D-12-00162.1.
414	Wernli, H., and C. Schwierz (2006), Surface cyclones in the ERA40 data set (1958-2001).
415	Part I: Novel identification method and global climatology, J. Atmos. Sci., 63, 2486-
416	2507, doi:10.1175/JAS3766.1.
417	Whan, K., F. Zwiers, and J. Sillmann (2016), The influence of atmospheric blocking
418	on extreme winter minimum temperatures in north america, J. Climate, (2016), doi:
419	10.1175/JCLI-D-15-0493.1.

-14-

- Wilks, D. S. (2011), Statistical Methods in the Atmospheric Sciences, International Geo-
- 421 *physics Series*, vol. 100, 3 ed., Elsevier Inc, doi:10.1016/B978-0-12-385022-5.00001-4.

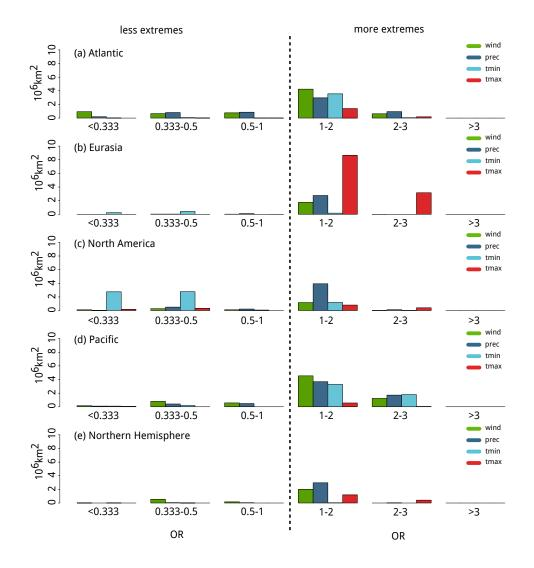


Figure 1. Land area north of 10 °N with statistically significant ORs of DJF wind (green), DJF precipitation (dark blue), DJF cold (light blue) and JJA hot (red) extremes for high waviness in the North Atlantic
(a), the Eurasian (b), the North American (c) and the North Pacific (d) sector and in the entire Northern
Hemisphere (e) for different OR categories.

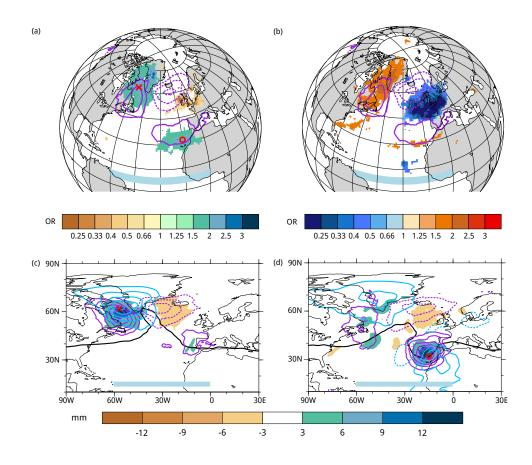


Figure 2. Statistically significant ORs of (a) precipitation and (b) wind gust extremes for high waviness 426 in the North Atlantic sector (indicated with light blue bars). Solid (dashed) purple contours depict positive 427 (negative) cyclone frequency anomalies for DJF high waviness days in the Atlantic sector in absolute per-428 centage points starting from 5pp (-5pp), every 5pp (-5pp). Panels (c) and (d) depict composites of various 429 variables for days when high waviness in the North Atlantic sector co-occurs with a precipitation extreme 430 at 57 °W/62 °N (c) and at 15 °W/32 °N (d): Precipitation anomaly relative to the DJF daily mean precipita-431 tion (shading), cyclone frequency anomaly as in (a,b) but starting from 10pp every 10pp, composite 2 PVU 432 contour (solid black) and standardized anomalies of the vertically integrated specific humidity in light blue, 433 starting at plus (solid) and minus (dashed) 0.5 standard deviation, every 0.5 standard deviation. Red crosses 434 and circles indicate the two grid points. 435

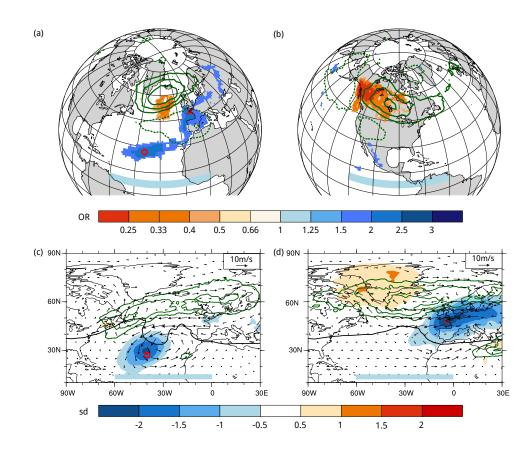
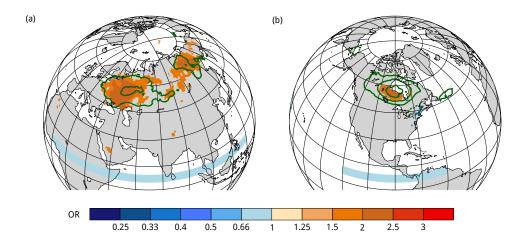


Figure 3. Statistically significant ORs of DJF cold extremes for high waviness in the (a) Atlantic and (b) 436 North American sector (sectors indicated with light blue bars in all panels). Solid (dashed) green contours 437 depict positive (negative) blocking frequency anomalies for DJF high waviness days in the respective sector in 438 absolute percentage points starting from 5pp (-5pp), every 5pp (-5pp). Panels (c) and (d) depict composites of 439 various variables for days when high waviness in the North Atlantic sector co-occurs with a precipitation ex-440 treme at 40  $^{\circ}W/27 ^{\circ}N$  (c) and at 4  $^{\circ}W/40 ^{\circ}N$  (d): Standardized 2 m temperature anomaly (shading), blocking 441 frequency anomaly as in (a,b) but starting from 10pp every 10pp, composite 2 PVU contour (solid black) and 442 wind anomalies at 850 hPa. Red crosses and circles indicate the two grid points. 443



**Figure 4.** Statistically significant ORs of JJA hot extremes for high jet waviness in the (a) Eurasian sector

- and (b) the North American sector. Green contours (blocking frequency anomaly) as in Figure 3. The blue bar
- depicts the extent of the respective sector.